

## Coupled optical interface modes in a Fibonacci dielectric superlattice

G. J. Jin and S. S. Kang

*Department of Physics and National Laboratory of Solid State Microstructures, Nanjing University, Nanjing 210093, People's Republic of China*

Z. D. Wang

*Department of Physics, The University of Hong Kong, Pokfulam Road, Hong Kong*

A. Hu and S. S. Jiang

*Department of Physics and National Laboratory of Solid State Microstructures, Nanjing University, Nanjing 210093, People's Republic of China*

(Received 25 March 1996; revised manuscript received 22 May 1996)

The coupled optical interface modes in a Fibonacci dielectric superlattice are studied. In the dielectric continuum approximation, the dispersion relation is found to have two bands of *dual triadic Cantor structures*, each being nonuniform scaling. For most of the eigenfrequencies, the amplitude profiles of electrostatic potential in this quasiperiodic structure are critical. Moreover, an invariant is analytically derived and is used to describe the general features of the frequency spectra and potential profiles. [S0163-1829(96)02742-7]

In recent years, there has been considerable interest in elementary excitations in artificial multilayers or superlattices.<sup>1-3</sup> In particular, the optical phonon problem in alkali halide or polar semiconductor superlattices is rather attractive.<sup>2</sup> Usually, the optical modes can be divided into two types: one is a type of bulklike excitations, the other is a type of interface mode. Interestingly, the interface modes will be coupled to give the collective excitation of the whole superlattice when the layer thickness of the system is relatively small. On the other hand, since the discovery of a quasicrystalline phase in Al-Mn alloys, great experimental and theoretical efforts have been devoted to physical properties in one-dimensional quasiperiodic structures.<sup>4-7</sup> As is well known, the quasiperiodicity of Fibonacci structure has substantial impact on the properties of elementary excitations. Therefore, it is worthwhile to explore the properties of coupled optical interface modes in Fibonacci dielectric superlattices. In this paper, we first derive the basic formulas for transfer matrices, an invariant, and the dispersion relation. Then the numerical results as well as relevant discussions are presented.

A Fibonacci superlattice is a simple one-dimensional quasiperiodic structure with two building blocks denoted by  $L$  and  $S$ . For the structures considered here, each of them is constructed by two layers with materials  $A$  and  $B$ . The  $B$  layers in  $L$  and  $S$  blocks have the same thickness  $d$ , but the  $A$  layers have thickness  $d_L$  in  $L$  blocks and  $d_S$  in  $S$  blocks, respectively. Using these two blocks, a Fibonacci dielectric superlattice is formed according to the rule:  $S_{j+1} = \{S_j, S_{j-1}\}, S_1 = L, S_2 = LS$ .  $A$  and  $B$  are two kinds of dielectric materials with different dielectric functions  $\epsilon_A$  and  $\epsilon_B$ , which are the same as those in the corresponding infinite media and may be frequency dependent.

In the electrostatic limit, the electrostatic potential  $\Phi$  satisfies the Laplace equation  $\nabla^2\Phi(\mathbf{r},t)=0$ . If the  $z$  axis is chosen to be perpendicular to the superlattice planes, without loss of generality, we assume that only a plane-wave

$\exp(ikx)$  propagates along the  $x$  direction with  $k$  as the in-plane wave vector. It is reasonable to write  $\Phi(\mathbf{r},t) = \phi(z)\exp\{i(kx - \omega t)\}$ , and thus,

$$\left(\frac{d^2}{dz^2} - k^2\right)\phi(z) = 0. \quad (1)$$

Denoting  $n$  as a layer index, the electrostatic continuum conditions at the interface takes the form

$$\phi_n(z) = \phi_{n+1}(z), \quad \epsilon_n \frac{d\phi_n(z)}{dz} = \epsilon_{n+1} \frac{d\phi_{n+1}(z)}{dz}. \quad (2)$$

The solutions of Eq. (1) can be written as  $\phi_l(z) = g_l e^{kz} + h_l e^{-kz}$  in the  $A$  layers, and  $\phi_l(z) = p_l e^{kz} + q_l e^{-kz}$  in the  $B$  layers, where  $l$  denotes the block index. If we write

$$\begin{pmatrix} g_{l+1} \\ h_{l+1} \end{pmatrix} = T_{l+1,l} \begin{pmatrix} g_l \\ h_l \end{pmatrix} \quad (3)$$

for  $A$  layers, it is straightforward to obtain

$$T_{l+1,l} = \begin{pmatrix} \alpha e^{k(d_{l+1}+d_l)/2} & \beta e^{k(d_{l+1}-d_l)/2} \\ -\beta e^{-k(d_{l+1}-d_l)/2} & \gamma e^{-k(d_{l+1}+d_l)/2} \end{pmatrix}, \quad (4)$$

where

$$\alpha = \cosh kd + \frac{1}{2} \left( \frac{\epsilon_B}{\epsilon_A} + \frac{\epsilon_A}{\epsilon_B} \right) \sinh kd, \quad (5)$$

$$\beta = \frac{1}{2} \left( \frac{\epsilon_B}{\epsilon_A} - \frac{\epsilon_A}{\epsilon_B} \right) \sinh kd,$$

$$\gamma = \cosh kd - \frac{1}{2} \left( \frac{\epsilon_B}{\epsilon_A} + \frac{\epsilon_A}{\epsilon_B} \right) \sinh kd.$$

One can find that there are three types of transfer matrices  $T_{L,L}$ ,  $T_{S,L}$ ,  $T_{L,S}$ , which are all unimodular. As usual, we set  $M_1 = T_{L,L}$  and  $M_2 = T_{L,S}T_{S,L}$ , and have recursion relations  $M_{j+1} = M_{j-1}M_j$ , from which all  $M_j$ 's can be obtained, where  $j$  is the Fibonacci generation number.

Defining  $\chi_j = \frac{1}{2}\text{Tr}M_j$ , one can find that the quantity  $I = \chi_{j+1}^2 + \chi_j^2 + \chi_{j-1}^2 - 2\chi_{j+1}\chi_j\chi_{j-1} - 1$  is invariant. For our Fibonacci dielectric superlattice,

$$I = \frac{1}{4} \left( \frac{\varepsilon_B}{\varepsilon_A} - \frac{\varepsilon_A}{\varepsilon_B} \right)^2 \sinh^2 k d \sinh^2 k (d_L - d_S). \quad (6)$$

This analytic formula is different from those for electrons and acoustic phonons in Fibonacci chains.<sup>8</sup> Comparing with that for magnetostatic modes in Fibonacci multilayers,<sup>6</sup> both invariants appear to have the same wave-vector dependence, but different frequency dependence. The invariant can be used to characterize the structure of energy spectra as well as the properties of the states of Fibonacci structures.<sup>8</sup>

In the calculation of the frequency spectra of Fibonacci dielectric superlattice, we here use the free-boundary condition: the electrostatic potentials at the left and the right boundaries, which contact with the environment of dielectric function  $\varepsilon_C$ , are  $\Phi_L$  and  $\Phi_R$  with  $\Phi_{L,R} = \phi_{L,R} \exp\{i(kx - \omega t)\}$ . In detail, the constraint equations are written as

$$\begin{aligned} (\varepsilon_A - \varepsilon_C) e^{-kd_L/2} g_1 - (\varepsilon_A + \varepsilon_C) e^{kd_L/2} h_1 &= 0, \\ (\varepsilon_A - \varepsilon_C) e^{kd_L/2} g_{N+1} - (\varepsilon_A + \varepsilon_C) e^{-kd_L/2} h_{N+1} &= 0. \end{aligned} \quad (7)$$

On the other hand, the global equation for the quasiperiodic structure can be written as

$$\begin{pmatrix} g_{N+1} \\ h_{N+1} \end{pmatrix} = M_j \begin{pmatrix} g_1 \\ h_1 \end{pmatrix} = \begin{pmatrix} m_{11} & m_{12} \\ m_{21} & m_{22} \end{pmatrix} \begin{pmatrix} g_1 \\ h_1 \end{pmatrix}, \quad (8)$$

where  $m_{11}$ ,  $m_{12}$ ,  $m_{21}$ , and  $m_{22}$  are all complicated functions of the wave-vector, thicknesses, and frequency. The linear equations of  $g_1$ ,  $h_1$ ,  $g_{N+1}$  and  $h_{N+1}$  in Eqs. (7) and (8) have nontrivial solutions only if the coefficient determinant vanishes. Thus the dispersion equation becomes

$$\begin{aligned} (\varepsilon_A^2 - \varepsilon_C^2) e^{2kd_L} m_{11} + (\varepsilon_A - \varepsilon_C)^2 e^{kd_L} m_{12} - (\varepsilon_A + \varepsilon_C)^2 e^{kd_L} m_{21} \\ - (\varepsilon_A^2 - \varepsilon_C^2) m_{22} = 0. \end{aligned} \quad (9)$$

Equation (9) is the central result of this paper, from which all relevant information regarding the optical interface modes in the present quasiperiodic structure can be extracted. We will see later on, in a specified case, this equation is of  $2F_j$ -th order in  $\omega$ , which gives  $2F_j$  eigenfrequencies for each value of  $k$ , where  $F_j$  is a Fibonacci number satisfying the relation  $F_j = F_{j-1} + F_{j-2}$  with  $F_1 = F_0 = 1$ .

Each of the eigenfrequencies can create a special distribution of potential. First, we consider the amplitudes in  $A$  layers. By using Eqs. (3) and (4), the potential amplitudes  $g_{l+1}, h_{l+1}$  of  $l+1$  block can be recursively obtained if  $g_1$  and  $h_1$  are known.<sup>9</sup> After  $g_l$  and  $h_l$  are determined, the potential distributions in the  $B$  layers, characterized by  $p_l$  and  $q_l$ , can also be obtained.

To get the concrete dispersion relation from Eq. (9), we choose  $\varepsilon_A$  as frequency independent, but  $\varepsilon_B(\omega) = \varepsilon_{B,\infty}(\omega^2$

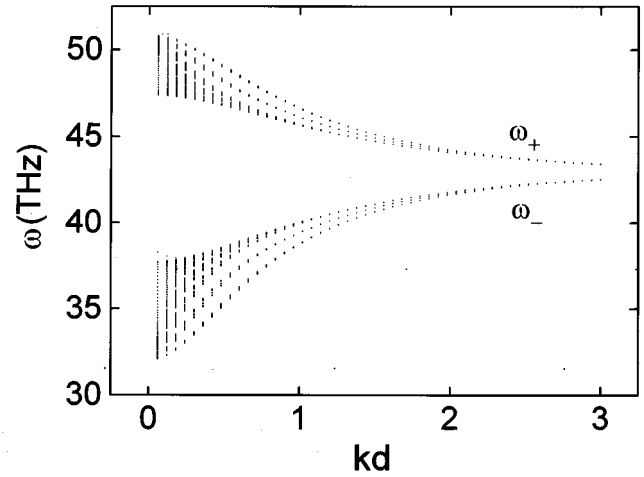


FIG. 1. Dispersion relation of the coupled optical interface modes for 12th order Fibonacci superlattice. Here  $d_L = 2d_S = 4d$ .

$-\omega_{B,LO}^2)/(\omega^2 - \omega_{B,TO}^2)$ , as for alkali halide or polar semiconductor materials, where  $\omega_{B,LO}$  and  $\omega_{B,TO}$  are the longitudinal- and transverse-optical frequencies. We take  $\varepsilon_A = 2.1$ , as the value of  $\text{SiO}_2$ ;  $\varepsilon_{B,\infty} = 2.34$ ,  $\varepsilon_{B,0} = 5.9$ ,  $\omega_{B,TO} = 32.01$  THz and  $\omega_{B,LO} = 50.74$  THz, which correspond to the values of NaCl;  $\varepsilon_C = 1$  (the value of vacuum).

Figure 1 shows the dispersion relation of coupled optical interface modes for 12th order Fibonacci dielectric superlattice, where  $d_L = 4d$ ,  $d_S = 2d$ , and  $d$  is fixed. The spectra are divided into two branches, namely  $\omega_+$  and  $\omega_-$ , which are separated by a gap as in the periodic superlattices.<sup>1</sup> For lower  $kd$ , the spectra form two bands, while for higher  $kd$ , the modes are highly degenerate. Between these two limits, being also different from periodic superlattices, there are many gaps to appear. It can be seen more clearly from Fig. 2 that the allowed frequencies form two branches of Cantor sets, which are singular continuous. For the  $j$ th order Fibonacci dielectric structure, the subbands of  $\omega_+$  or  $\omega_-$  have  $F_{j-2}, F_{j-1}, F_{j-2}$  eigenfrequencies, respectively. One can

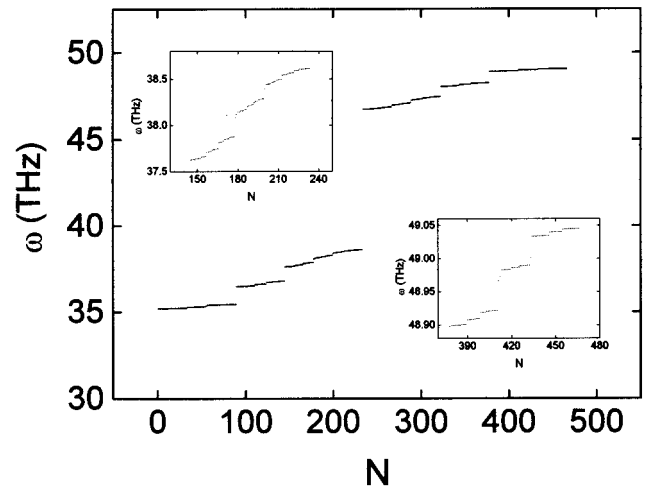


FIG. 2. Eigenfrequency versus number of modes for a 12th order Fibonacci superlattice with  $kd_L = 2.0$ ,  $kd_S = 1.0$ , and  $kd = 0.5$ . Two enlarged local regions are shown in the insets.

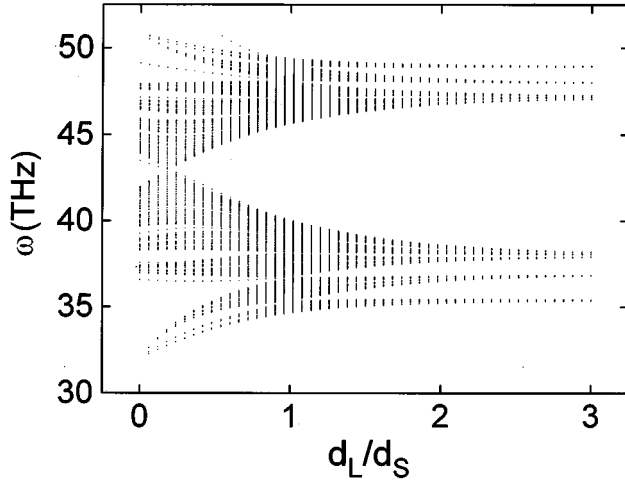


FIG. 3. The variation of eigenfrequency distribution with the thickness ratio  $d_L/d_S$  for  $kd_S=1.0$  and  $kd=0.5$ .

also see that for the  $\omega_+$  band, the low-frequency subband is wider than high-frequency subband, but for the  $\omega_-$  band, the situation is reversed. This feature reflects the strength of quasiperiodicity, as can be illustrated by Eq. (6): the lower region of the  $\omega_-$  band and the higher region of the  $\omega_+$  band have larger values of  $I$ , while the higher region of  $\omega_-$  band and the lower region of the  $\omega_+$  band have smaller values of  $I$ .

The relative thicknesses of  $d$ ,  $d_L$ , and  $d_S$  have important effects on the frequency spectra. One example is shown in Fig. 3. When  $k$ ,  $d_S$  and  $d$  are fixed ( $kd_S=1.0, kd=0.5$ ), the frequency spectra are all threefold branches as  $d_L/d_S \neq 1$ . Notice that, for  $d_L/d_S \rightarrow 1$ , two continuous bands are prominent, which stems from the fact that the structure becomes periodic (at this time  $I \rightarrow 0$  as expected). However, the quasiperiodicity is more prominent for small or large values of  $d_L/d_S$ . Particularly for very large  $d_L/d_S$ , the spectra become six highly degenerate branches, which seem to be different from the existing results in the literatures. For example, when  $d_L/d_S \gg 10.0$ , numerical calculations show that

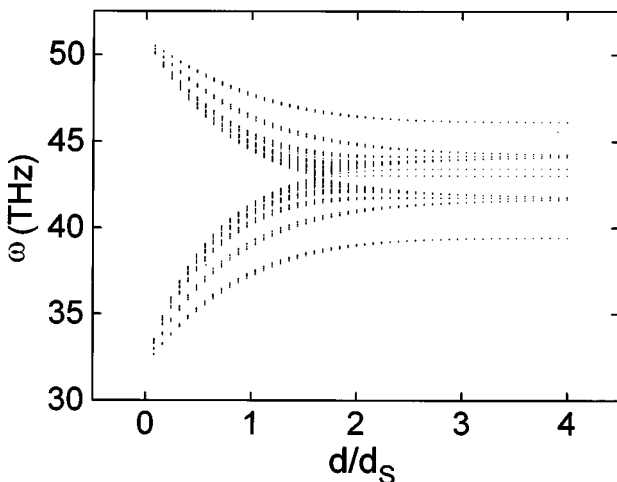


FIG. 4. The variation of eigenfrequency distribution with the thickness ratios  $d/d_S$  for  $kd_L=2.0$  and  $kd_S=1.0$ .

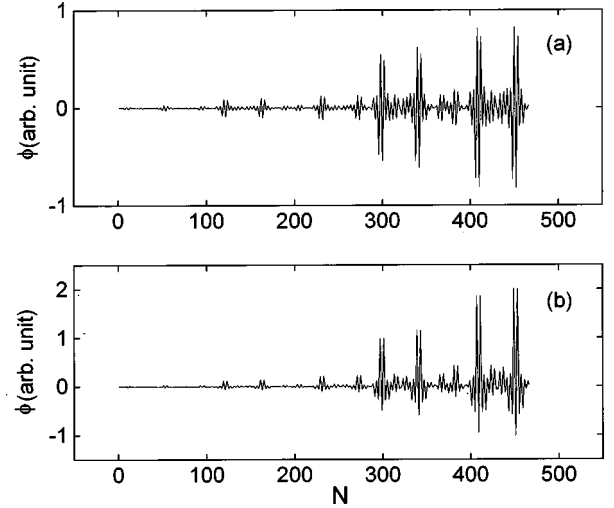


FIG. 5. The amplitude profiles of electrostatic potential for two critical states: (a)  $\omega=35.218\ 148\ 127\ 7$ ; (b)  $\omega=49.040\ 631\ 708\ 8$ .

there are only six limiting frequencies  $\omega = 35.388\ 308\ 194\ 9$ ,  $36.862\ 657\ 159\ 6$ ,  $38.023\ 154\ 200\ 9$ ,  $47.175\ 283\ 229\ 3$ ,  $47.985\ 416\ 306\ 7$ ,  $48.936\ 159\ 968\ 8$ . These six limiting frequencies are the isolated modes when the thickness  $d_L$  approaches infinity; they are actually the solutions of the following three equations:

$$\begin{aligned} \varepsilon_B^2 + 2\varepsilon_A\varepsilon_B\coth kd + \varepsilon_A^2 &= 0, \\ (1 - e^{-kd_S})\varepsilon_B^2 + 2\varepsilon_A\varepsilon_B\coth kd + (1 + e^{-kd_S})\varepsilon_A^2 &= 0, \\ (1 + e^{-kd_S})\varepsilon_B^2 + 2\varepsilon_A\varepsilon_B\coth kd + (1 - e^{-kd_S})\varepsilon_A^2 &= 0. \end{aligned} \quad (10)$$

Figure 4 shows another example, where  $k$ ,  $d_L$  and  $d_S$  are fixed ( $kd_L=2.0$  and  $kd_S=1.0$ ). For  $d/d_S \ll 1$ , the eigenfrequencies approach  $\omega_{B,LO}$  and  $\omega_{B,TO}$ , while for  $d/d_S \gg 1$ , there also exist six limiting frequencies  $\omega =$

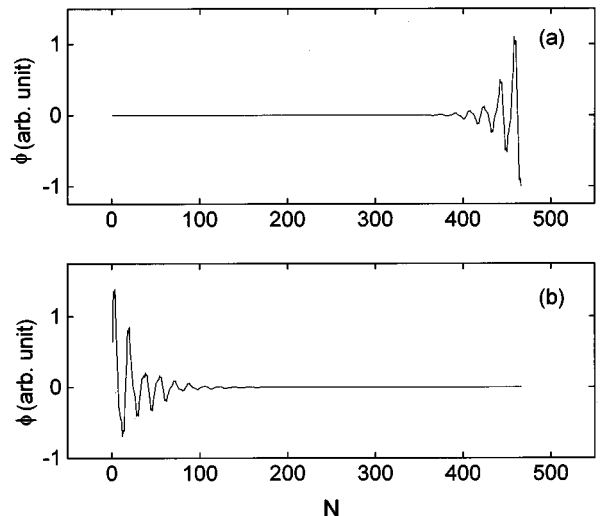


FIG. 6. The amplitude profiles of electrostatic potential for two quasilocalized states corresponding to the band-edge frequencies: (a)  $\omega=38.085\ 539\ 634\ 3$ ; (b)  $\omega=38.119\ 253\ 211\ 6$ .

39.427 153 712 9, 41.716 274 108 1, 43.026 124 350 3, 43.430 412 732 0, 44.165 714 517 2, 46.114 221 825 4 corresponding to another kind of isolated modes, which satisfy another set of equations

$$\varepsilon_B = -\varepsilon_A \tanh kd_S, \quad \varepsilon_B = -\varepsilon_A \coth kd_S, \\ \varepsilon_B = -\varepsilon_A \tanh kd_L, \quad \varepsilon_B = -\varepsilon_A \coth kd_L, \quad (11)$$

$$\varepsilon_B = -\varepsilon_A \frac{\varepsilon_A \tanh kd_L + \varepsilon_C}{\varepsilon_A + \varepsilon_C \tanh kd_L}, \quad \varepsilon_B = -\varepsilon_A \frac{\varepsilon_A \tanh kd_L - \varepsilon_C}{\varepsilon_A - \varepsilon_C \tanh kd_L}.$$

The quasiperiodicity of the frequency spectra must be reflected in the distribution of potential which is related to the long-wavelength optical oscillations. If the averaged potential over each layer is considered, then

$$\phi_l^A = (g_l + h_l) \sinh(kd_l) / (kd_l/2) \quad (12)$$

for the  $A$  layers, and

$$\phi_l^B = \frac{1}{kd} \left\{ \left[ \sinh kd + \frac{\varepsilon_A}{\varepsilon_B} (\cosh kd - 1) \right] e^{kd_l/2} g_l \right. \\ \left. + \left[ \sinh kd - \frac{\varepsilon_A}{\varepsilon_B} (\cosh kd - 1) \right] e^{-kd_l/2} h_l \right\}, \quad (13)$$

for the  $B$  layers. For the parameters chosen in Fig. 2, we have examined all potential profiles of  $2F_{12}=466$  eigenfre-

quencies and find that almost all states are critical. This fact can be illustrated by the values of the invariant which range from 0.465 068 026 2 to 4.355 134 986 3. Figures 5(a) and 5(b) show two critical states corresponding to  $N=13$ , 454 modes in Fig. 2. The potential profiles in these two figures obey power laws, which is quite similar to the cases of tight-binding electrons, acoustic phonons or magnetostatic spin waves; but it is interesting to note that  $N=454$  mode is the 13th mode counted from the upper part of the  $\omega_+$  band. The similarity of these two states denotes the *duality* of the  $\omega_-$  and  $\omega_+$  bands, which is specific to the present system, in contrast to the well-studied systems.<sup>3-6</sup> Actually, almost all the states for these two bands are one to one correspondent in overall characteristics, although there may be some differences in detail.

Among the 466 states, still a few states are quasilocalized. These states usually appear at the edges of the subbands in Fig. 2. Figures 6(a) and 6(b) are two examples. Their frequencies are corresponding to the  $N=178$ , 179 modes, and both modes are at the two sides of a gap. These two states are localized at the surfaces of the superlattices: one at the left and the other at the right, and both are symmetric. Here the duality of the  $\omega_+$  band and  $\omega_-$  band also exists.

This work was supported by the National Natural Science Foundation of China, the Provincial Natural Science Foundation of Jiangsu, and the RGC of Hong Kong under Grant No. HKU262/95P.

- <sup>1</sup>R. E. Camley and D. Mills, Phys. Rev. B **29**, 1695 (1984); B. L. Johnson and R. E. Camley, *ibid.* **38**, 3311 (1988).  
<sup>2</sup>C. Colvard, T. A. Gant, M. V. Klein, R. Merlin, R. Fischer, H. Morkoc, and A. C. Gossard, Phys. Rev. B **31**, 2080 (1985); A. K. Sood, J. Menéndez, M. Cardona, and K. Ploog, Phys. Rev. Lett. **54**, 2115 (1985); E. P. Pokatilov and S. I. Beril, Phys. Status Solidi B **110**, K75 (1982); Kun Huang and Bangfen Zhu, Phys. Rev. B **38**, 13 377 (1988).  
<sup>3</sup>R. E. Camley, T. S. Rahman, and D. L. Mills, Phys. Rev. B **27**, 261 (1983); P. Grünberg and K. Mika, *ibid.* **27**, 2955 (1983).  
<sup>4</sup>M. Kohmoto and J. R. Banavar, Phys. Rev. B **34**, 563 (1986); F. Nori and J. P. Rodriguez, *ibid.* **34**, 2207 (1986).  
<sup>5</sup>P. Hawrylak and J. J. Quinn, Phys. Rev. Lett. **57**, 380 (1986); B. L. Johnson and R. E. Camley, Phys. Rev. B **44**, 1225 (1991); N.

- H. Liu, Y. He, W. G. Feng, and X. Wu, *ibid.* **52**, 11 105 (1995).  
<sup>6</sup>J. W. Feng, G. J. Jin, A. Hu, S. S. Kang, S. S. Jiang, and D. Feng, Phys. Rev. B **52**, 15 312 (1995).  
<sup>7</sup>R. Merlin, K. Bajema, R. Clarke, F.-Y. Juang, and P. K. Bhattacharya, Phys. Rev. Lett. **55**, 1768 (1985); M. W. C. Dharma-wardana, A. H. MacDonald, D. J. Lockwood, J.-M. Barkeau, and D. C. Houghton, *ibid.* **58**, 1761 (1987); K. Bajema and R. Merlin, Phys. Rev. B **36**, 4555 (1987); A. Hu, C. Tien, X. Li, Y. Wang, and D. Feng, Phys. Lett. A **119**, 313 (1986); X.-K. Zhang, H. Xia, G.-X. Cheng, A. Hu, and D. Feng, *ibid.* **136**, 312 (1989).  
<sup>8</sup>M. Kohmoto, B. Sutherland, and C. Tang, Phys. Rev. B **35**, 1020 (1987).  
<sup>9</sup>J. E. S. Socolar and P. J. Steinhardt, Phys. Rev. B **34**, 617 (1986).